Bulk High-Impact Polystyrene Process, 1

Partitions of *tert*-Butyl Peroctoate and Styrene in Blends Containing Polystyrene and a Rubber

Carla V. Luciani, Diana A. Estenoz, Gregorio R. Meira,*
Nancy L. García, Haydée M. Oliva

In relation to the bulk high-impact polystyrene process, this work investigates the partition between phases of styrene and an initiator: *tert*-butyl peroctoate. A Flory-Huggins model was applied for predicting the phase separation point and the partitions of styrene and *tert*-butyl peroctoate. For blends of styrene, polystyrene, and a styrene-butadiene diblock copolymer, the model provides reasonable predictions of a ternary equilibrium diagram. For blends of styrene, polystyrene, polybutadiene, and *tert*-butyl peroctoate, the partition of *tert*-butyl peroctoate was measured at 25 °C. At emulated conversions of 13% or lower, equilibrium was reached after 1 h of mixing time. For the higher molar masses and conversion of 16%, equilibrium was not reached after 24 h of mixing time. To fit the equilibrium measurements, the solubility parameter of *tert*-butyl peroctoate was adjusted.

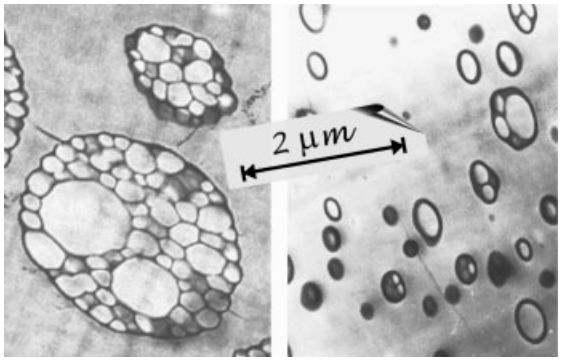

Introduction

High-impact polystyrene (HIPS) is a heterogeneous material of rubber particles dispersed in a continuous free polystyrene (PS) matrix. It is produced by polymerizing styrene (St) in the presence of a rubber such as polybutadiene (PB) or a St-butadiene (Bd) block copolymer (BC). Most of the initial PB chains are grafted along the polymerization, yielding a St-Bd graft copolymer (GC). The final material contains approximately 80% free PS and 20% GC.[1]

In a typical bulk (or quasi-bulk) HIPS process, St is polymerized in the presence of 5–10 wt.-% of PB and a chemical initiator (I) along the following stages: dissolution, prepolymerization, finishing, and devolatilization. The process has been crudely represented by straight lines in ternary St/PS/PB diagrams;[2–6] Figure 1 reproduces one of such diagrams by Casís et al.,[5] where the binodal curve and tie lines were in turn taken from Kruse at 60 °C.[4] After dissolving the PB in St, the prepolymerization starts at Point A (Figure 1). Initially, the reaction is homogeneous, but it phase-separates at a monomer conversion in the range 0.5–2% (Point B).[2–5] Between the phase separation and the phase inversion (Point C), the continuous phase is PB-rich, and the disperse phase is PS-rich. After the phase inversion, the PS-rich phase remains as the continuous phase.

C. V. Luciani, D. A. Estenoz, G. R. Meira
INTEC (Universidad Nacional del Litoral and CONICET), Güemes 3450, Santa Fe (S3000GLN), Argentina
Fax: 54-342-455-0944; E-mail: gmeira@ceride.gov.ar
N. L. García, H. M. Oliva
Escuela de Ingeniería Química, Universidad del Zulia, Maracaibo, Venezuela

DOI: 10.1002/mats.200700036

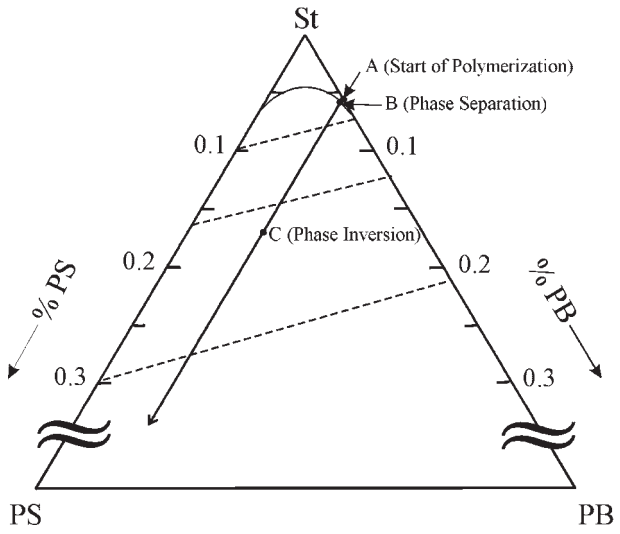

Figure 1. Phase diagram of a ternary St/PS/PB blend at 60 °C, adapted from Casís et al.[5] The arrow represents the reaction path of a polymerization of St in the presence 6 wt.-% of PB, where rubber grafting is neglected.

The rubber particle morphology is basically developed along the phase inversion period. The final rubber particles are generally heterogeneous, with vitreous PS occlusions. In "core-shell" morphologies, each of the (relatively small) rubber particles contains a single (but relatively large) PS occlusion. In "salami" morphologies, the larger rubber particles contain multiple occlusions. Most of the chemical initiator is consumed during the prepolymerization, with the aim of inducing an early rubber grafting. The finishing stage is gently stirred (to avoid destroying the developed particle morphology), and carried out at a higher temperature (to promote thermal St initiation and to reduce the viscosity). In the devolatilization stage, the solvent and unreacted monomer are separated from the polymer. The final HIPS properties are essentially determined by the particle morphology and the molecular weights of the continuous PS matrix.[7–10]

The distribution between phases of the low molar mass species (St and I) is quantified through the following partition coefficients:[4,11,12]

$$K_{St} = \frac{[St]_2}{[St]_1} \quad (1)$$

$$K_I = \frac{[I]_2}{[I]_1} \quad (2)$$

where subscripts 1 and 2 indicate the PS-rich and PB-rich phases, respectively. The investigated process presents a formidable challenge for measuring such partition coefficients. This is because: i) blending experiments that emulate the polymerization process are limited to room temperatures (since even in the absence of an initiator, it is impossible to avoid the thermal St polymerization); ii) the generated GC reduces the interfacial tension and makes it difficult to separate the phases by centrifugation decantation; iii) the phase volumes and species concentrations vary continuously along the reaction; and, iv) the initial initiator concentration is below the detection limits of standard spectroscopic techniques.

The partitions of St and several initiators have been measured at room temperature in blends with PS and PB, but avoiding the presence of GC.[4,11,12] Ludwico and Rosen[11] measured the partitions of St and 2 initiators 2,2′-azoisobutyronitrile (AIBN) and benzoyl peroxide (BPO) at 0 and 25 °C, in blends containing 5 wt.-% of PB and a series of St/PS ratios. While all the partition coefficients were close to 1, St showed a slight preference for the PB-rich phase ($K_{St} > 1$), and the opposite was observed for the initiators ($K_I < 1$).[11] In addition, the partitions were little affected by the temperature, the initiator concentrations, and the emulated conversions.[11] Similarly, Bertin et al.[12] measured the partition coefficients of several commercial peroxides (3 percarbonates, a perester, and a perketal) in St/PS/PB/initiator blends; emulating conversions up to the phase inversion. As before, all the coefficients were close to unity; showing a weak dependence with the initiator concentrations and emulated conversions.[12]

Several articles[4,13–17] have simulated the thermodynamic equilibrium of St/PS/PB blends by means of the Flory-Huggins theory,[13] which calculates the excess of free-energy due to entropic and enthalpic contributions. The enthalpic terms are a function of the chemical interactions between the different species and such interactions have been assumed binary and temperature-dependant in the case of ternary St/PS/PB blends.[4,16,17]

This article is the first in a series that investigates the partition of an initiator (*tert*-butyl peroctoate, TBPO) in blends with St, PS, and a rubber. A mathematical model was developed. First, it was applied to estimate the partition of St in blends with PS and a St-Bd block copolymer. Then, experiments were carried out with the blend St/PS/PB/TBPO, and a single model parameter was adjusted.

In the second article of this series,[18] the partition model is combined with a heterogeneous polymerization model for calculating the partition of St and initiator and phase separation point along a bulk polymerization of St in the presence of PB, taking into account that most of the original PB is transformed into a graft copolymer. In the third article of this series,[19] the model is further extended for predicting the average rubber particle morphology developed after the phase inversion.

Macromol. Theory Simul. **2007**, *16*, 703–710

Macromolecular Journals
DOI: 10.1002/mats.200700036

Partition Model for St/PS/Rubber/I Blends

Consider the partition of St and an initiator in blends with PS and a rubber (R) that can be either PB or a St-Bd BC. After the phase separation, the model assumes complete incompatibility between the PS and PB homopolymers, but partial miscibility between the free PS and the BC.[4,11,13,20] Thus, in St/PS/PB/I blends, the PS-rich phase is composed of St, PS, and I, while the PB-rich phase is composed of St, PB, and I. In the case of St/PS/BC/I blends, all four chemical species were assumed present in both phases.[20]

For each of the chemical species (i = St, PS, R, and I), their mass balances are:

$$G_i = G_{i,1} + G_{i,2}; \quad (i = \mathrm{St, PS, R, I}) \tag{3}$$

where G_i is the total mass of species i, and $G_{i,j}$ is the mass of species i in phase j (= 1, 2). Due to the incompatibility between PS and PB chains, it is $G_{PS,2} = G_{PB,1} = 0$. The volumes of the PS-rich and rubber-rich phases (V_1 and V_2, respectively) are estimated from:

$$V_j = \sum_i \frac{G_{i,j}}{\rho_i}; \quad (j = 1, 2;\ i = \mathrm{St, PS, R, I}) \tag{4}$$

where ρ_i is the bulk density of species i.

After the phase separation, the chemical species reach equilibrium when their chemical potentials in the PS-rich phase are equal to their chemical potentials in the rubber-rich phase:

$$\mu_{i,1} = \mu_{i,2} \quad (i = \mathrm{St, PS, R, I}) \tag{5}$$

According to Flory-Huggins,[13] Equation (5) can be written as follows:

$$\begin{aligned} &\ln\left(\frac{\phi_{i,1}}{\phi_{i,2}}\right) + \sum_k \chi_{k,i}(\phi_{k,1} - \phi_{k,2}) - 1/2 \\ &\quad \times \sum_k \sum_m \chi_{k,m}(\phi_{k,1}\phi_{m,1} - \phi_{k,2}\phi_{m,2}) \\ &\quad - \sum_k \frac{\phi_{k,1} - \phi_{k,2}}{r_k} \\ &= 0; \\ &(i, k, m = \mathrm{St, PS, R, I}) \end{aligned} \tag{6}$$

with:

$$\phi_{i,j} = \frac{G_{i,j}/\rho_i}{\sum_k G_{k,j}/\rho_k}; \quad (i, k = \mathrm{St, PS, R, I};\ j = 1, 2) \tag{7}$$

where $\phi_{i,j}$ is the volume fraction of species i in phase j; $\chi_{k,i}$ is the binary interaction parameter between species k and i; and, r_i is a variable that depends on the molar mass and density of species i.

For St, PS, PB, and I, the variables r_i are given by:[17,21]

$$r_i = \frac{\hat{\rho}_{\mathrm{St}}}{\hat{\rho}_i}\overline{r}_{\mathrm{n},i}; \quad (i = \mathrm{St, PS, PB, I}) \tag{8}$$

where $\hat{\rho}_i$ is the molar density of species i (for the homopolymers, it is expressed in moles of repetitive units per unit volume); and, $\overline{r}_{\mathrm{n},i}$ is the number-average chain length (for the low molar mass species, it is $\overline{r}_{\mathrm{n,St}} = \overline{r}_{\mathrm{n,I}} = 1$). In addition, the binary interaction parameters $\chi_{k,i}$ between species St, PS, PB, and I, are:[4,22–24]

$$\begin{aligned} &\chi_{k,i} = 0.34 + \frac{(\delta_k - \delta_i)^2}{\hat{\rho}_k \mathrm{RT}}; \\ &\quad (k = \mathrm{St, I};\ i = \mathrm{St, PS, PB, I}) \end{aligned} \tag{9}$$

where δ_{St}, δ_{I}, δ_{PS}, and δ_{PB} are the solubility parameters of St, I, PS, and PB, respectively.

For the BC, r_i is calculated assuming additive contributions from each of its blocks:[17]

$$r_{\mathrm{BC}} = \frac{\hat{\rho}_{\mathrm{St}}}{\hat{\rho}_{\mathrm{PS}}}\overline{s}_{\mathrm{n,BC}} + \frac{\hat{\rho}_{\mathrm{St}}}{\hat{\rho}_{\mathrm{PB}}}\overline{b}_{\mathrm{n,BC}} \tag{10}$$

where $\overline{s}_{\mathrm{n,BC}}$ and $\overline{b}_{\mathrm{n,BC}}$ are the number-average chain lengths of the PS and PB blocks, respectively. Finally, the interaction parameters between the BC and the other species ($\chi_{\mathrm{BC,St}}$, $\chi_{\mathrm{BC,I}}$, $\chi_{\mathrm{BC,PS}}$, and $\chi_{\mathrm{BC,PB}}$) were estimated from the homopolymer binary parameters and the average mass fraction of St in the BC ($\overline{w}_{\mathrm{St,BC}}$), as follows:[17]

$$\begin{aligned} \chi_{\mathrm{BC,i}} &= \overline{w}_{\mathrm{St,BC}}\chi_{\mathrm{PS,i}} + (1 - \overline{w}_{\mathrm{St,BC}})\chi_{\mathrm{PB,i}} \\ &\quad - \overline{w}_{\mathrm{St,BC}}(1 - \overline{w}_{\mathrm{St,BC}})\chi_{\mathrm{PS,PB}}; \\ &(i = \mathrm{St, PS, PB, I}) \end{aligned} \tag{11}$$

The partition model is given by Equation (3)–(9) for R = PB, and by Equation (3)–(11) for R = BC. The model inputs are the temperature; the total masses of St, PS, R, and I (G_i); the (number-average) chain lengths of PS and R ($\overline{r}_{\mathrm{n,PS}}$, $\overline{r}_{\mathrm{n,R}}$); and the average mass fraction of St when the rubber is a BC ($\overline{w}_{\mathrm{St,BC}}$). The model outputs are the phase volumes (V_j) and the masses of chemical species in each of the phases ($G_{i,j}$). From these results, the partition coefficients can be estimated through:

$$K_i = \frac{G_{i,2}}{G_{i,1}}\frac{V_1}{V_2}; \quad (i = \mathrm{St, I}) \tag{12}$$

Table 1. Partition model parameters.

Parameter	Value			Reference
	25 °C	90 °C	120 °C	
δ_{PS} ($J^{1/2} \cdot cm^{-3/2}$)	17.4	17.4	17.4	[23]
δ_{PB} ($J^{1/2} \cdot cm^{-3/2}$)	18.8	18.8	18.8	[23]
δ_{St} ($J^{1/2} \cdot cm^{-3/2}$)	19.0	19.0	19.0	[24]
ρ_{St} ($kg \cdot m^{-3}$)	900.8	841.1	813.5	[24]
ρ_{PS} ($kg \cdot m^{-3}$)	1 069.7	1 030.3	1 012.2	[23]
ρ_{PB} ($kg \cdot m^{-3}$)	893.5	856.5	840.8	[22]
$\chi_{PS,PB}$	0.187	0.117	0.092	[25]
δ_{TBPO} ($J^{1/2} \cdot cm^{-3/2}$)	11.6	11.6	11.6	Adjusted in this work
ρ_{TBPO} (kg/m^3)	900	900	900	Producer Data

For any fixed initial St/R ratio, the phase separation point was determined by increasing the PS/St ratios until all calculated compositions were positive real numbers. (During the initial homogeneous period of low PS/St ratios, some of the predicted concentrations are represented by negative or complex numbers.) For blends that lack one or more of the base species, the equations of their corresponding mass and chemical potential balances should be eliminated.

The algebraic system of equations was solved through a Newton-Raphson numerical technique. The model parameters are presented in Table 1. The interaction parameter between PS and PB ($\chi_{PS,PB}$), and the solubility parameters of St, PS, and PB (δ_{St}, δ_{PS}, δ_{PB}, respectively) were directly taken from the literature.[23–25] Unfortunately however, the solubility parameters of most chemical initiators are unknown, and must be adjusted to experimental data.

Application Examples

Estimation of Ternary St/PS/BC Diagrams

White and Patel[20] investigated several St/PS/Rubber blends at 20 °C, and Figure 2 reproduces the equilibrium measurements of: i) a St/PS/BC blend with $\overline{M}_{n,PS} = 80\,000$;[20] $\overline{M}_{w,PS}/\overline{M}_{n,PS} = 3$;[20] $\overline{M}_{n,BC} = 52\,000$;[26] $\overline{M}_{w,BC}/\overline{M}_{n,BC} = 1.5$,[26] and $\overline{w}_{St,BC} = 0.25$;[26] and ii) a St/PS/PB blend with the same PS characteristics, but with $\overline{M}_{n,PB} = 69\,000$[20] and $\overline{M}_{w,PB}/\overline{M}_{n,PB} = 3.4$.[20] The measurements were determined by visual examination of the phase-separated layers, and did not include an estimation of the corresponding tie lines. As expected, the St/PS/BC blend exhibits a wider homogeneous region than the St/PS/PB blend, due to the increased compatibilization introduced by the PS block.

Consider the simulation of the St/PS/BC measurements of Figure 2. In this case without initiator, all the model parameters were directly taken from the literature (Table 1). The model predictions include the binodal curve and corresponding tie lines. The binodal curve was calculated by adopting different initial BC contents and increasing the PS/St ratios until phase separation was detected. Then, the tie lines were obtained by adopting different global compositions inside the (lower) heterogeneous region, and calculating the corresponding phase compositions. For the 2 measurements on the right-hand side, the model predicts phase separations at PS/St ratios lower than those actually observed. Possible reasons for the observed deviations are: a) the interaction parameters were assumed to depend

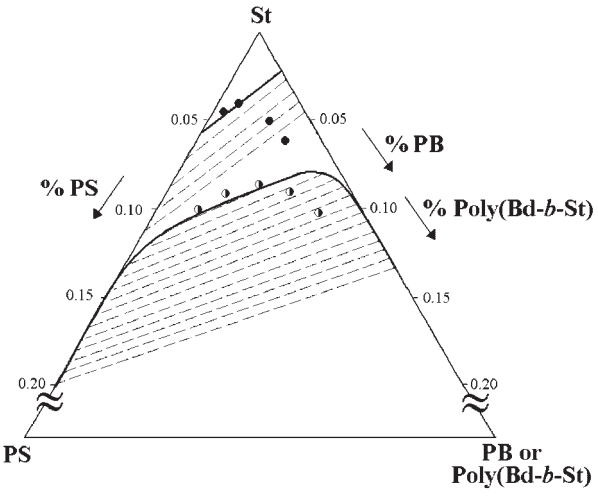

Figure 2. Phase diagram at 20 °C of measurements by White and Patel[20] corresponding to a ternary St/PS/BC blend (lower section) (◑); and to a St/PS/PB system (upper section) (●). The model predictions include the binodal curves (continuous trace), and the corresponding tie lines (dashed trace).

Macromol. Theory Simul. **2007**, *16*, 703–710

Macromolecular Journals

DOI: 10.1002/mats.200700036

only on temperature and solubility parameters, but not on the phase compositions; b) all the parameters were directly taken from the literature; and, c) the model assumes incompatibility between PS and PB chains, thus generating an overestimated incompatibility between free PS and BC. This last reason explains the shape of the predicted binodal curve, that rapidly becomes too close (and tangent) to the St/PS and St/BC axes. The slopes of the tie lines indicate a preferential accumulation of St in the BC/St phase. This is because the solubility parameter of St (δ_{St}) is closer to that of PB (δ_{PB}) than to that of PS (δ_{PS}) (Table 1).

Consider the simulation of the St/PS/PB measurements of Figure 2. Due to the complete incompatibility assumption between PS and PB chains, the model predicts a linear binodal curve. Thus, the model is clearly inadequate for simulating systems that contain relatively large mass fractions of PB homopolymer.

Partition of TBPO in St/PS/PB/TBPO Blends

Experimental Work

TBPO is a typical initiator of the bulk HIPS process.[1,27] Sixteen experiments were carried out for determining the partition of TBPO in St/PS/PB/TBPO blends. The experimental conditions are in the first 4 columns of Table 2. They involved combinations of 2 base PS samples (PS_h and PS_l), 2 blending times (24 and 1 h), and 4 emulated conversions ($x = 9$, 13, 16, and 20%). In all the experiments, the temperature was 25 °C and the global concentrations of TBPO and PB were fixed at 5 $g \cdot L^{-1}$ and 6 wt.-%, respectively. The long blending times of Experiment 1–4 and 9–12 were aimed at ensuring equilibrium conditions. The short blending times of Experiment 5–8 and 13–16 were adopted to emulate a typical mean residence time of a continuous industrial prepolymerization reactor.[1,27]

The St monomer, the (medium-cis) PB, and the TBPO were kindly provided to us by Estizulia C.A. (Maracaibo, Venezuela). The 2 base PS samples were synthesized in our laboratories at 2 different temperatures (PS_h at 70 °C, and PS_l at 120 °C). The polymerizations were carried out in a 2 L stainless-steel reactor with stirring rate 250 rpm, pressure 5 atm, and total reaction time 24 h. The monomer was vacuum-distilled (over $AlLiH_4$). All the average molecular weights (Table 2) were determined by size exclusion chromatography (SEC), in a Waters ALP/GPC 244 chromatograph fitted with a refractive index detector

Table 2. Determination of the initiator partition coefficients in St/PS/PB/TBPO blends. In all the experiments, the temperature was 25 °C, and the global concentrations of TBPO and the medium cis PB[a] were 5 $g \cdot L^{-1}$ and 6 wt.-%, respectively.

Experiment	Base PS	Blending Time	Emulated Conversion x	PS-Rich Phase		PB-Rich Phase		K_{TBPO}
				V_1	$c_{I,1}$	V_2	$c_{I,2}$	
		h	%	mL	$g \cdot L^{-1}$	mL	$g \cdot L^{-1}$	
1	PS_h[b]	24	9	4.3	5.93	6.6	4.41	0.74
2	PS_h[b]	24	13	6.2	5.58	4.6	4.26	0.76
3	PS_h[b]	24	16	6.5	5.11	4.3	4.81	0.95
4	PS_h[b]	24	20	7.4	5.19	3.3	4.64	0.88
5	PS_h[b]	1	9	4.4	5.89	5.51	4.36	0.74
6	PS_h[b]	1	13	5.8	6.38	3.67	4.85	0.76
7	PS_h[b]	1	16	6.6	3.89	3.38	6.56	1.70
8	PS_h[b]	1	20	7.2	4.53	2.52	6.39	1.33
9	PS_l[c]	24	9	5.8	5.45	5.1	4.51	0.82
10	PS_l[c]	24	13	6.3	5.44	4.6	4.33	0.78
11	PS_l[c]	24	16	7.0	5.31	3.8	4.39	0.84
12	PS_l[c]	24	20	7.9	5.35	2.7	4.22	0.78
13	PS_l[c]	1	9	5.5	5.44	4.12	4.57	0.82
14	PS_l[c]	1	13	6.7	5.42	3.66	4.29	0.78
15	PS_l[c]	1	16	7.3	4.52	2.94	6.15	1.35
16	PS_l[c]	1	20	7.8	4.90	2.00	5.50	1.10

[a]PB: $\overline{M}_n = 141\,000$ and $\overline{M}_w = 283\,000$; [b]$PS_h$: $\overline{M}_n = 328\,000$ and $\overline{M}_w = 1\,033\,000$; [c]$PS_l$: $\overline{M}_n = 227\,000$ and $\overline{M}_w = 671\,000$.

and a complete set of μStyragel Waters columns (10^2, 10^3, 10^4, 10^5, and 10^6 Å).

The main experiments were carried out as follows: i) PS was added into St and stirred for 1 h until complete dissolution; ii) the (fixed amount of) PB was added, and the mixture was stirred for about 4 h until complete dissolution; iii) the (fixed amount of) liquid TBPO was added, and the mixtures (of about 90 mL) were stirred at 250–500 rpm with a Heidolph R6170 impeller for either 24 or 1 h; iv) samples of approximately 10 mL were centrifuged at 6 000 rpm, until clear decantation; v) the PS-rich and PB-rich phase volumes (V_1 and V_2, respectively) were directly determined from the calibrated centrifuge tubes (see Table 2); vi) the upper phase was carefully extracted by means of a syringe, and centrifugation was repeated when re-mixing was observed; and, vii) the TBPO concentrations in each of the phases were measured by IR spectrophotometry.

The FTIR spectrophotometer was a Perkin Elmer 1710 with a NaCl window cell for liquids. The TBPO concentration was quantified through the C=O stretching at 1 770 cm^{-1}. The sample cell had to be opened and washed after every spectrum measurement. For this reason, the optical paths of the empty cell were determined before each spectrum measurement, through an interference pattern technique. The extinction coefficients of TBPO in the PS-rich and PB-rich phases were estimated from calibration curves obtained with standard solutions of St/PS/TBPO and St/PB/TBPO, yielding: $\alpha_1 = 2.79\ cm^2 \cdot g^{-1}$ in the PS-rich phase and $\alpha_2 = 3.47\ cm^2 \cdot g^{-1}$ in the PB-rich phase. Finally, the TBPO concentrations were calculated through the Lambert-Beer law, from the measured absorbances and optical paths. The TBPO concentrations were determined by triplicate, and the final averages are given in Table 2, under $c_{I,1}$ and $c_{I,2}$.

The final partition coefficients are in the last column of Table 2 and in Figure 3(a). In the 24 h experiments, TBPO showed a slight preference for the PS-rich phase ($K_{TBPO} < 1$); and this result is in accord with previous measurements by Ludwico and Rosen[11] for benzoyl peroxide. At conversions of 9 and 13%, the results of the 1 h experiments were almost coincident with those of the 24 h experiments, and were quite independent of the PS molar mass. This suggests a fast mass transfer of TBPO between phases at the lower system viscosities. In contrast, for conversions of 16 and 20%, large differences are observed between the 24 h and 1 h experiments, and between the experiments with PS_l and PS_h. This suggests that equilibrium may have not been reached, even in 24 h experiments (Figure 3(a)). Furthermore, at 16 and 20% conversion, all the K_{TBPO} values are much larger than unity, with a maximum of 1.70 for Experiment 7 (with PS_h and blending time 1 h). Possible explanations are: i) the reduced diffusivities of TBPO at the higher system viscosities; and ii) an eventual presence of a third (initiator droplets) phase that remained dispersed in the PB-rich phase.

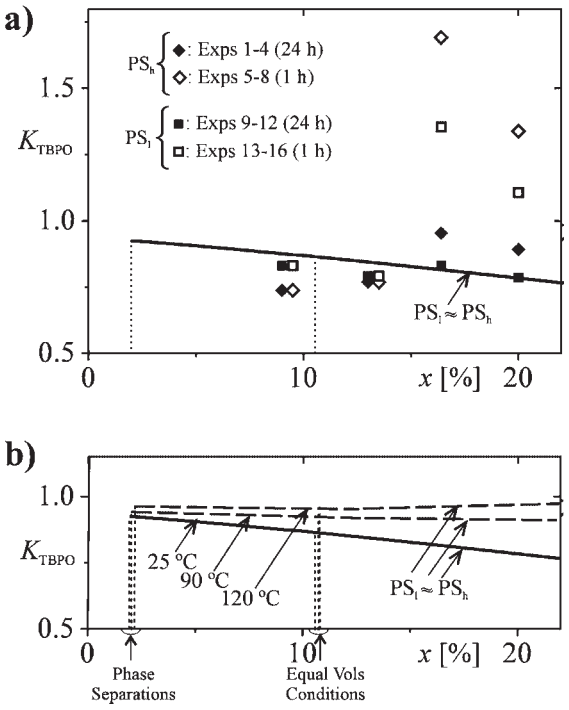

Figure 3. a) Partition coefficients of TBPO at 25 °C in St/PS/PB/TBPO blends. The experiments involved 2 PS samples, 2 blending times, and 4 emulated conversions (Table 2). The measurements are represented by symbols and the model predictions are represented by a continuous trace. A model parameter was adjusted to the 24 h experiment measurements. According to the model, the phase separation occurs at $x \cong 1.9\%$, the equal volumes condition occurs at $x \cong 10.4\%$, and the partitions are almost independent of the PS molar mass. b) The model predictions for K_{TBPO} at 25 °C (continuous trace) are compared with the model predictions at 90 and 120 °C (dashed trace).

Model Predictions

Consider now the partition model predictions. The solubility parameter of TBPO (δ_{TBPO}) could not be found in the literature, and it was adjusted to the 24 h experiment results. The adjustment was carried out by means of an iterative Nelder-Mead[28] algorithm, which minimized the difference between measurements and model predictions. The resulting δ_{TBPO} is presented in Table 1. According to the adjusted model (Figure 3(a)), the phase separation occurs at $x \approx 1.9\%$, and this value is in accord with literature data.[4,11,20] The equal volume condition (at $x \approx 10.4\%$) has been adopted as an indication of the phase inversion point.[3,5] The predicted equal volume condition is in accord with the volume phase measurements of Table 2. Also, the simulation results suggest that the TBPO partitions are almost unaffected by the PS molecular weights (Figure 3(a)).

Macromol. Theory Simul. **2007**, *16*, 703–710

DOI: 10.1002/mats.200700036

Finally, Figure 3(b) presents the model predictions for the TBPO partitions at 90 and 120 °C (i.e., at 2 typical pre-polymerization temperatures). According to the model, the values of K_{TBPO} are increased at such higher temperatures, and become closer to unity. In addition, the model predicts negligible variations in the phase separation points and equal volume conditions, and a negligible effect of the PS molar mass. Even though not shown in Figure 3, when employing a low molar mass PS (of $\overline{M}_{n,PS} = 10\,000$), the predicted K_{TBPO} values were seen to be reduced by only 5%.

Conclusion

The Flory-Huggins theory[13] was applied for estimating the distribution of St and an initiator in blends with PS and a rubber (either PB or BC). For a St/PS/BC blend, quite acceptable model predictions were obtained, in spite of the fact that model parameters were directly taken from the literature. Experiments with St/PS/PB/TBPO blends at room temperature showed that at low emulated conversions (of 9 and 13%), the TBPO partition coefficient was almost independent of the blending times and of the PS molar masses; thus indicating a rapid mass transfer and thermodynamic equilibrium. In contrast, at high emulated conversions (of 16 and 20%), the partition coefficient measurements were greatly affected by the blending times and the PS molar masses; suggesting that large errors could be introduced in the bulk polymerization models when assuming an instantaneous distribution of species.

Nomenclature

BC	Block copolymer
$\overline{b}_{n,BC}$	Number-average chain length of the PB block contained in the BC, dimensionless
G_i	Total mass of species i (i = St, PS, R, I), g
$G_{i,j}$	Mass of species i (i = St, PS, R, I) in phase j (j = 1, 2), g
I	Initiator
K_k	Partition coefficient of species k (k = St, I) between the PB-rich and PS-rich phases, dimensionless
$\overline{M}_{n,i}$	Number-average molar mass of species i (i = PS, R), $g \cdot mol^{-1}$
$\overline{M}_{w,i}$	Weight-average molar mass of species i (i = PS, R), $g \cdot mol^{-1}$
PB	Polybutadiene
PS	Polystyrene
R	Rubber (either PB or the BC)
$\overline{r}_{n,i}$	Number-average chain length of species i (i = St, PS, R, I), dimensionless
$\overline{s}_{n,BC}$	Number-average chain length of the PS block contained in the BC, dimensionless
St	Styrene
T	Temperature, K
V_j	Volume of phase j (j = 1, 2), L
$\overline{w}_{St,BC}$	Average mass fraction of St in the BC
x	Monomer conversion, %

Greek Symbols

$\chi_{i,k}$	Binary interaction parameter between species i and k (i, k = St, PS, R, I) dimensionless
δ_i	Solubility parameter of species i (i = St, PS, R, I), $J^{1/2} \cdot cm^{-3/2}$
$\phi_{i,j}$	Volume fraction of species i (i = St, PS, R, I) in phase j (j = 1, 2), dimensionless
$\mu_{i,j}$	Chemical potential of species i (i = St, PS, R, I) in phase j (j = 1, 2), $J \cdot mol^{-2}$
ρ_i	Density of species i (i = St, PS, R, I), $g \cdot L^{-1}$
$\hat{\rho}_i$	molar density of species i (i = St, PS, R, I), $mol \cdot L^{-1}$

Acknowledgements: The authors acknowledge the financial support by *Universidad Nacional del Litoral*, *CONICET*, *ANPCyT*, *Universidad del Zulia*, *CONDES-LUZ*, and our *CONICET-FONACIT* international agreement.

Received: May 29, 2007; Revised: August 8, 2007; Accepted: August 13, 2007; DOI: 10.1002/mats.200700036

Keywords: heterogeneous polymers; high-impact polystyrene; partition coefficients; phase separation; *tert*-butyl peroctoate

[1] D. A. Estenoz, G. R. Meira, N. Gómez, H. M. Oliva, *AIChE J.* **1998**, *44*, 427.
[2] W. A. Ludwico, S. L. Rosen, *J. Appl. Polym. Sci.* **1976**, *14*, 2121.
[3] M. Fischer, G. P. Hellmann, *Macromolecules* **1996**, *29*, 2498.
[4] R. L. Kruse, *Adv. Chem. Ser.* **1975**, *142*, 141.
[5] N. Casís, D. A. Estenoz, L. M. Gugliotta, H. M. Oliva, G. R. Meira, *J. Appl. Polym. Sci.* **2006**, *99*, 3023.
[6] N. Casís, D. A. Estenoz, J. R. Vega, G. R. Meira, *J. Appl. Polym. Sci.* **2007**, submitted.
[7] C. B. Bucknall, *Br. Plastics* **1967**, 118.
[8] G. Cigna, S. Matarrese, G. F. Biglione, *J. Appl. Polym. Sci.* **1976**, *20*, 2285.
[9] S. G. Turley, H. Keskkula, *Polymer* **1980**, *21*, 466.
[10] J. H. Choi, K. H. Ahn, S. Y. Kim, *Polymer* **2000**, *41*, 5229.
[11] W. A. Ludwico, S. L. Rosen, *J. Appl. Polym. Sci.* **1975**, *19*, 757.

[12] D. Bertin, F. Coutand, M. Duc, C. Galindo, D. Gigmès, S. Marque, P. Tordo, B. Vuillemin, *e-Polymer* **2004**, *10*, 1.
[13] P. J. Flory, "*Principles of Polymer Chemistry*", Cornell University Press, London 1953, p. 541.
[14] K. M. Hong, J. Noolandi, *Macromolecules* **1981**, *14*, 736.
[15] T. Inoue, T. Soen, T. Hashimoto, H. Kawai, *Macromolecules* **1970**, *3*, 87.
[16] R. J. Roe, W. C. Zin, *Macromolecules* **1980**, *13*, 1221.
[17] J. Noolandi, K. M. Hong, *Macromolecules* **1982**, *15*, 482.
[18] C. V. Luciani, D. A. Estenoz, G. R. Meira, *Macromol. Theory Simul.* **2007**, to be submitted.
[19] C. V. Luciani, D. A. Estenoz, G. R. Meira, *Macromol. Theory Simul.* **2007**, to be submitted.
[20] J. L. White, R. D. Patel, *J. Appl. Polym. Sci.* **1975**, *19*, 1775.
[21] C. H. Kang, S. I. Sandler, *Fluid Phase Equilibr.* **1987**, *38*, 245.
[22] R. P. Danner, M. S. High, "*Handbook of Polymer Solution Thermodynamics*", American Institute of Chemical Engineering, New York 1993, p. 38.
[23] J. F. Rudd, "Physical Constant of Poly(styrene)", in: *Polymer Handbook*, 3rd edition, J. Brandrup, E. H. Immergut, Eds., John Wiley & Sons, New York 1989, p. V/81.
[24] R. C. Reid, J. M. Prausnitz, T. K. Sherwood, "*The Properties of Gases and Liquids*", 3rd edition, McGraw-Hill, New York 1977, p. 26.
[25] H. Retsos, I. Margiolaki, A. Messaritaki, S. H. Anastasiadis, *Macromolecules* **2001**, *34*, 5295.
[26] T. Kotaka, J. L. White, *Macromolecules* **1974**, *7*, 106.
[27] C. V. Luciani, D. A. Estenoz, H. M. Oliva, G. R. Meira, *Ind. Chem. Eng. Res.* **2005**, *44*, 8354.
[28] J. A. Nelder, R. A. Mead, *Comput. J.* **1965**, *7*, 308.

Macromolecular Journals
DOI: 10.1002/mats.200700036